An elastic solution for the stress field at the tip of a Mode II propagating fatigue crack

M. W. Brown
Department of Mechanical Engineering, University of Sheffield, Sheffield (U.K.)
michaelbrown256@btinternet.com

ABSTRACT. It is notoriously difficult to achieve experimentally stable shear mode crack propagation in Mode II. The elastic stress field around a sharp elliptical crack is examined, using the classical solution of Inglis and Savin, and it is compared to the linear elastic fracture mechanics solution to reveal some important shortcomings of the latter approximate singular solution. Graphs of the characteristic stress field around a blunt crack are presented for Modes I and II. The crack tip radius of curvature and the size of the fatigue failure process zone required for stable shear mode cracking are discussed.

KEYWORDS. Elastic crack tip stress field; Fatigue crack propagation; Linear elastic fracture mechanics; Mode I; Mode II; Blunt cracks; Process zone size.

INTRODUCTION

A number of people have attempted to study Mode II, shear fatigue crack growth over the past forty years, but many failed because they observed that the crack branches to propagate in Mode I, an opening mode. However a few have achieved Mode II propagation successfully, particularly Otsuka [1]. In this paper we explore the crack tip stress fields for both Mode I and II loading, and draw conclusions about pertinent and necessary conditions for stable Mode II growth.

As an example, at Sheffield we attempted to study Mode II in a rail steel using a tubular specimen with a spark-eroded axial crack, tested in reversed torsion but with a superimposed constant compressive axial stress to stabilise the shear mode of growth. A similar experiment of Otsuka using mild steel was successful using an asymmetric four point bending method. But the Sheffield tests always produced branch cracks, even with axial compression as high as yield to close any incipient Mode I branch. The spark-eroded starter notch had a root radius of curvature of 0.08 mm (no pre-cracking was possible with this particular geometry); consequently as shown below the shear stress at the crack tip for Mode II loading was absolutely zero. Therefore no shear mode fatigue crack growth was generated in the absence of cyclic shear stresses.

However in engineering practice, shear mode cracking is not uncommon, and it is certainly important. In rail steel under rolling contact for high speed trains operating in a temperate climate, rail cracks are generated and extend just below the running surface on a plane of maximum cyclic shear stress, Fig. 1. In the presence of rain water, a small amount of fluid entrapped in the crack prevents crack closure, so that the Mode II displacements are not attenuated by friction between the crack faces. In drier conditions, friction prevails, and the crack then branches, either upwards leading to a loss of material from the rail surface, or more seriously downwards leading to a rail fracture [2]. So the reduction or elimination of frictional effects that attenuate crack sliding displacements is the first requirement for stable shear mode propagation.

Further reported examples of Mode II fatigue cracking are found in fretting fatigue, in Aluminium Lithium alloys, in roller bearings, in Stage I small fatigue cracks, in tests with sequential mixed mode load histories, and in torsion, particularly for low cycle fatigue. These correspond to short cracks below the Mode I threshold, microstructures that favour local shear deformation bands, compressive stress fields that close incipient tensile cracks, crystallographic cracks on a single flat

plane avoiding roughness induced closure, and a small tensile load cycle prior to a shear cycle to leave a residual crack opening avoiding closure, respectively. The final case is illustrated in Fig. 2, that in torsion cracks often follow shear planes in low cycle fatigue where the extensive plasticity and reduced levels of tensile stress favour the shear mode [3]. Even where Mode I cracking starts on 45^{O} planes, a transition to shear mode is seen for low cycle fatigue in a medium carbon steel.

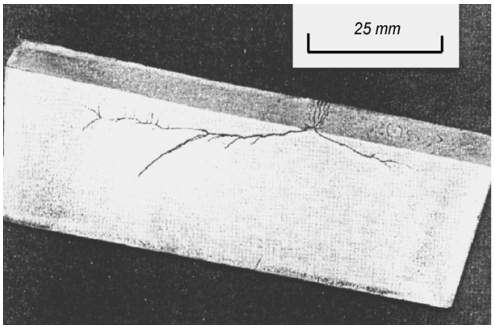

Figure 1: A squat fatigue crack in a rail line, which initiated from the running surface (top surface) and propagated on a shear plane, also showing tensile mode branches [2]. The rolling contact wheel travels from right to left.

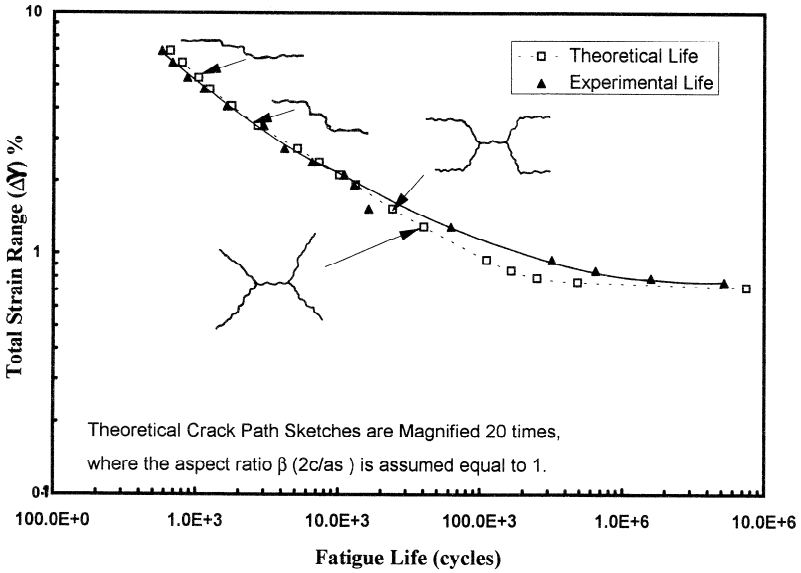

Figure 2: Torsional fatigue endurance curve for a medium carbon steel [3]. The crack shapes shown are sketched from real specimens, with the specimen axis horizontal. The theoretical curve was found by integration of crack propagation rules for tensile and shear modes of growth [3].

MODEL FOR TWO DIMENSIONAL CRACK TIP STRESS FIELDS

Real cracks are always are always blunt if we look closely enough at the crack tip. In continuum mechanics we usually assume a sharp crack where a singularity is formed at the crack tip, and using Lagrangian coordinates (where the initial singular geometry is maintained for the small strain case) the usual linear elastic fracture mechanics solution is derived. Even for an elastic solid, this gives an infinite strain on approaching the crack tip which is clearly not small, and the tip deforms into a parabolic shape for Mode I. Clearly we need to use Eulerian coordinates to allow for the changing geometry, and the singularity disappears, even for the smallest levels of applied load. A simpler alternative approach is to use the solutions for stresses around an elliptical notch due to Inglis [4], or Savin [5], and set the root radius of curvature of the sharp ellipse to match the crack tip curvature – for example calculated to match one half of

the crack opening displacement. These two dimensional plane stress solutions for a crack in an infinite plate are linear elastic, and do not need to use the approximations associated with the linear elastic fracture mechanics approach.
Details of the solution method of Savin [5] are presented elsewhere [6], for a plate under biaxial applied stress, with stress axes at a selected angle **α** with respect to the crack plane. The method provides a full field solution of the stress around an elliptical hole, assuming only linear elastic behaviour. Thus the results should be more accurate than the fracture mechanics approach, if we get the crack tip radius of curvature right, and if the crack can be sensibly modelled by a rather flat ellipse. The applied principal stresses are **S** and **ΛS** shown in Fig. 3. The stress tensors along a vector **t** at an angle **φ** measured from the crack tip are then evaluated for a range of **t** values. For this paper, the half crack length **D** was 10 mm, the ellipse half height **b** was 0.001 mm, giving a root radius of curvature **rho** of 10^{-7} mm. (In a steel with 350 MPa yield stress, this would correspond to about 20 MPa applied Mode I stress, but the actual stress level **S** is immaterial as the results are normalised.) Stresses are presented for a Cartesian coordinate system, where the y-axis is normal to the crack.

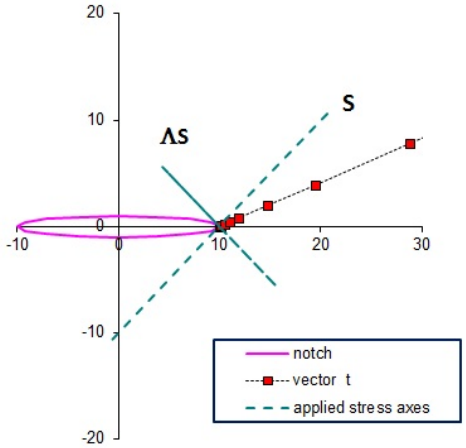

Figure 3: An elliptical notch in an infinite plate. The applied stresses S and ΛS have the first principal stress at an angle α to the horizontal in the Savin solution [6].

In the graphs that follow, the axes are normalised, and it transpires that for this normalisation scheme, the results are independent of applied stress and crack geometry in the crack tip region. On the horizontal axis, distance from the crack tip **t** is normalised by radius of curvature **rho**. (For an ellipse, **rho** = $\mathbf{b^2/D}$.) The stresses **sigma x, sigma y, and tau xy** (i.e. normal stress on x- and y-axes, and the shear stress) are each normalised by **Kt S** where **Kt** is defined as the stress concentration factor for a tensile stress normal to the crack, that is

$$\mathbf{Kt = 1 + 2.\sqrt{(D/rho)} - \Lambda}$$

Note this formula was used for the Mode II results as well as Mode I, as it characterises the crack tip geometry and the influence of curvature. It is not equal to the stress concentration factor in pure shear, nor in any other mixed mode case.
An Excel spreadsheet was developed with the Savin solution, and a second with the Inglis solution to ensure that they were identical. Results are presented for Mode I loading in Figs. 4 and 5, and for Mode II loading (pure shear) in Figs. 6 and 7. In these figures the linear elastic fracture mechanics (LEFM) results are also given, shown as dashed lines. Although a logarithmic scale is employed for the horizontal axis, the vertical scale is linear to permit negative stresses to appear.
Fig. 4 presents Mode I stresses, and there is clearly good agreement of the Savin solution with LEFM for **t/rho** greater than 10. For the far field (beyond 10^7), the LEFM stresses will fall to zero, being a first order asymptotic solution, whereas the Savin stress will approach the applied stress field. The LEFM results also deviate from reality at small values of **t/rho**, as they tend to infinity. However **sigma x** tends to zero, and **sigma y/(Kt S)** tends to a finite value of unity, governed by the stress concentration factor. It is also notable that **sigma x** peaks at **t = rho**. The LEFM analysis requires that the stresses **sigma x** and **sigma y** are equal on the x-axis (with a zero T-stress), but no such restriction applies for the Savin solution.
Fig. 5 covers the same situation as Fig. 4, but stresses are given for a $\varphi = 45^{O}$ line emanating from the crack tip. Again for **t/rho** greater than 10 LEFM works well. Both **sigma x** and **tau xy** fall to zero at the crack tip, as they must on meeting a vertical free surface at the blunt crack tip. As before **sigma y** remains finite.

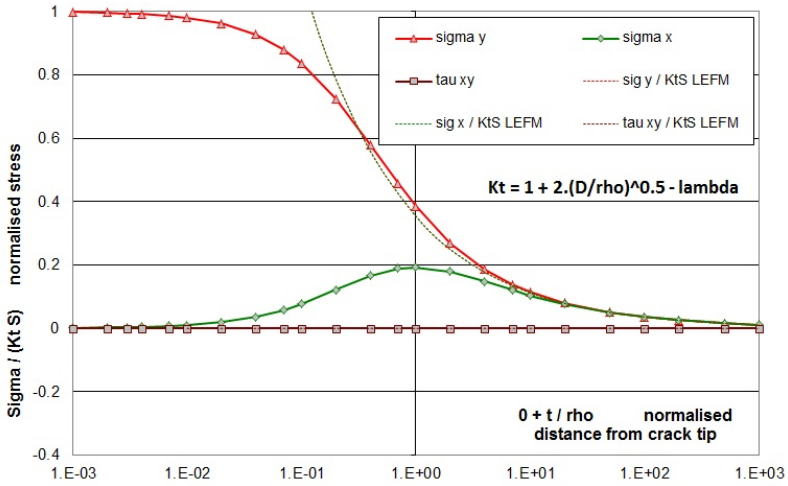

Figure 4: Mode I stresses ahead of the crack tip. Here $\Lambda = 0$, $\alpha = 90^{O}$, $\phi = 0^{O}$, **D** = 10 mm, **b** = 0.001 mm, **rho** = 10^{-7} mm. The stress **tau xy** is of course zero, from symmetry. The stresses **sigma x** and **sigma y** are equal for LEFM.

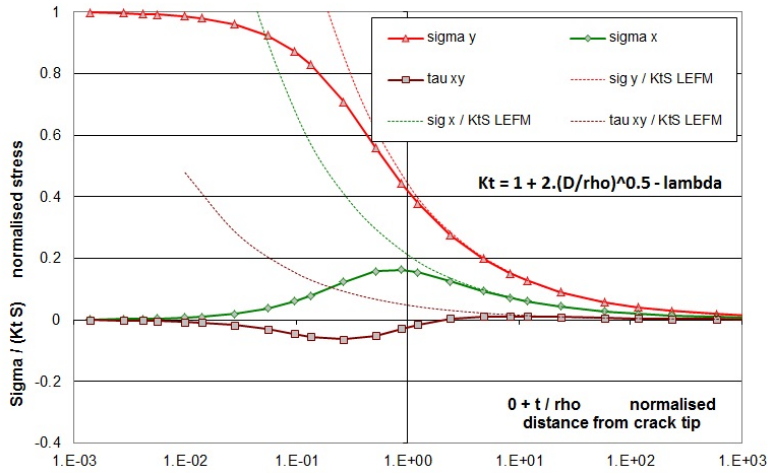

Figure 5: Mode I stresses on a 45^{O} plane emanating from the crack tip. Here $\Lambda = 0$, $\alpha = 90^{O}$, $\phi = 45^{O}$, **D** = 10 mm, **b** = 0.001 mm, **rho** = 10^{-7} mm.

Thus we see that close to the crack tip, if we can measure stresses in this region we should not try to model them by conventional fracture mechanics. Departures of LEFM results from reality are significant. Nevertheless, further from the crack tip the LEFM results are excellent, and very much easier to determine than the Savin technique. One should also note that the role of a plastic zone at the crack tip has not been taken into account, although it can easily be done by judicious choice of the radius of curvature, using for example the Dugdale model.

Having learnt how to interpret these graphs for the Mode I case, we can now look at Mode II, or indeed any mixed mode case, the role of T-stress, etc. Fig. 6 shows Mode II stresses ahead of the crack tip. Both LEFM and Savin predict that the only non-zero stress is **tau xy**, and even this falls to zero at the crack tip (although LEFM goes for an infinite value). Here we see one solution to the crack growth in torsion problem posed in the introduction. At the critical point where a shear mode crack should initiate, all three stresses are absolutely zero, so a shear fatigue crack has no driving force at all, even though LEFM predicts a healthy range of stress intensity factor. But this cannot be the full solution to our problem, because where Sheffield failed to grow a shear crack, Otsuka succeeded.

Overall, the Savin approach using blunt cracks appears to provide much better guidance to the near tip stress fields, and particularly in Mode II. It is worth pointing out that even though we do not have significant crack opening in shear, real cracks are blunt, and must have a radius of curvature of at least 5 to 10 Angstrom, or three atomic dimensions. If the

"crack tip" is only one atomic dimension wide, then we don't really have a crack, but an edge dislocation. So shear cracks should be treated as blunt cracks in an engineering world.

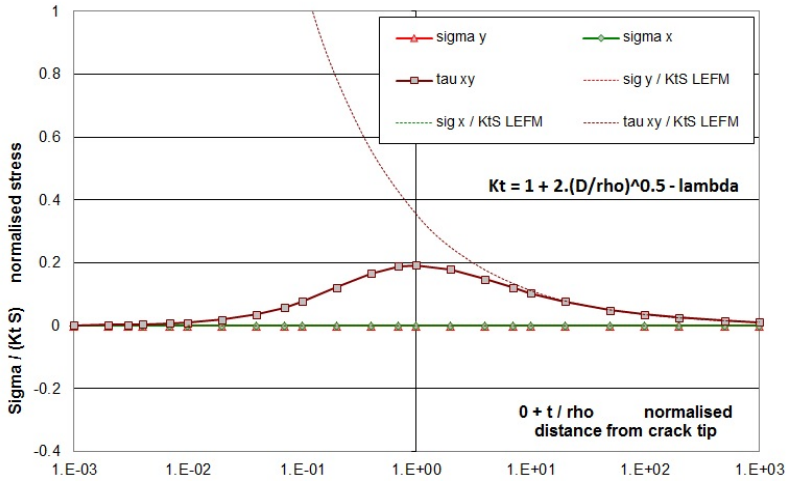

Figure 6: Mode II stresses ahead of the crack tip in pure shear. Here $\Lambda = -1$, $\alpha = 45^{O}$, $\phi = 0^{O}$, **D** = 10 mm, **b** = 0.001 mm, and **rho** = 10^{-7} mm. The stresses **sigma x** and **sigma y** are of course zero, from symmetry.

Fig. 7 presents the Mode II shear case, but stresses are given for a $\phi = 45^{O}$ line emanating from the crack tip. Again all stresses fall to zero at the crack tip, whereas the LEFM solution makes all stresses infinite. Peak stresses values are found subsurface, at a distance of one radius of curvature from the notch root. LEFM should only be used after ten radii of curvature from the crack tip.

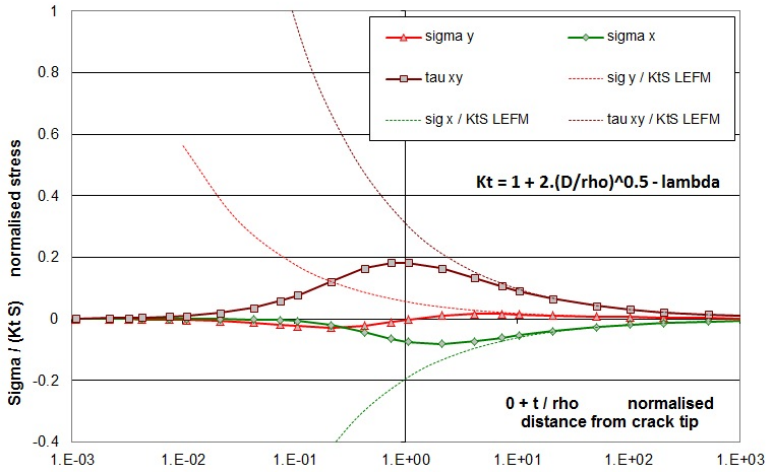

Figure 7: Mode II stresses on a 45^{O} plane emanating from the crack tip in pure shear. Here $\Lambda = -1$, $\alpha = 45^{O}$, $\phi = 45^{O}$, **D** = 10 mm, **b** = 0.001 mm, and **rho** = 10^{-7} mm.

FATIGUE FAILURE PROCESS ZONE

Clearly Mode II shear cracks can propagate under the right conditions, as discussed in the Introduction. One way, probably the only way to explain this is to introduce the concept of a process zone. This should not be confused with the plastic zone, which corresponds with a zone of cyclic deformation that is essential to developing and controlling the fatigue damage process. However apart from cyclic (and reversible) deformation, we also need a crack tip region where failure or decohesion can take place. This region is far smaller than the plastic, with dimensions much the

same as the crack growth increment per cycle. It is about equal to the crack tip opening displacement of a growing crack, or twice the radius of curvature. We can call this the "fatigue failure process zone".
In Fig. 7, the curves plotted are a repeat of Fig. 5 for stresses ahead of a shear crack, but with two potential fatigue failure processes zones added. The smaller zone falls in the region of zero or low stress, and therefore corresponds to non-propagating shear cracks. All a crack can do is branch to follow a tensile mode path, as observed in the "Sheffield" experiments. This non-propagating condition was all but inevitable because of the large radius of curvature of the spark-eroded starter crack. A process zone (or crack growth rate) of order 0.1 mm would be required for shear mode growth, which is far too big to be practical. Hence branching is observed in practice.
However in Otsuka's test, a four point bending sample was used, and this permits pre-cracking in fatigue, in simple bending to produce a sharp initial fatigue crack. With a much smaller crack tip radius of curvature, the fatigue failure process zone appears as the larger example in Fig. 7. So long as the zone extends beyond the peak in shear stress in the figure, then the intensified stress can interact with the failure process, and shear mode growth can occur. The intensity of stress can be calculated by integrating the shear stress over the zone to obtain an average value, and that provides the driving force for fatigue failure.

DISCUSSION AND CONCLUSIONS

It has been demonstrated that the Savin solution can provide the full field of stresses around the crack tip, so long as the radius of curvature at the crack tip can be identified. Some shortcomings of LEFM have been identified, which can explain the difficulty of predicting growth of shear mode cracks, unless the intensity of stress is correctly identified. Radius of curvature can be calculated from the Dugdale model for crack tip opening displacement, for Mode I. Even for Mode II, in the Introduction it was seen that a degree of crack opening is needed for frictionless crack face sliding, so this can be used to estimate the radius of curvature for real cracks.
Fig. 8 is worth discussing, as it points towards a method to make the Savin technique more acceptable as a practical procedure. This is essentially the same as Fig. 4, but the vertical axis is logarithmic. Secondly a constant factor of 0.25 has been added to the dimensionless factor plotted on the abscissa. This factor was chosen arbitrarily to make the line for normal stress straight, with a slope of -0.5.
Also in the figure, there are results for five different ellipse semi-widths, while **D** is kept constant at 10 mm. For **b** = 10 mm, we have a circular hole rather than a crack like defect. Semi-widths of 1, 0.1, 0.01, 0.001 mm all fit the same unique line for the near tip stress field, diverging from the line only for the far field response. So a simplified fit to the stress field is possible here. Stress equations will be functions of the angle φ, as well as the non-dimensional parameters in the figure.

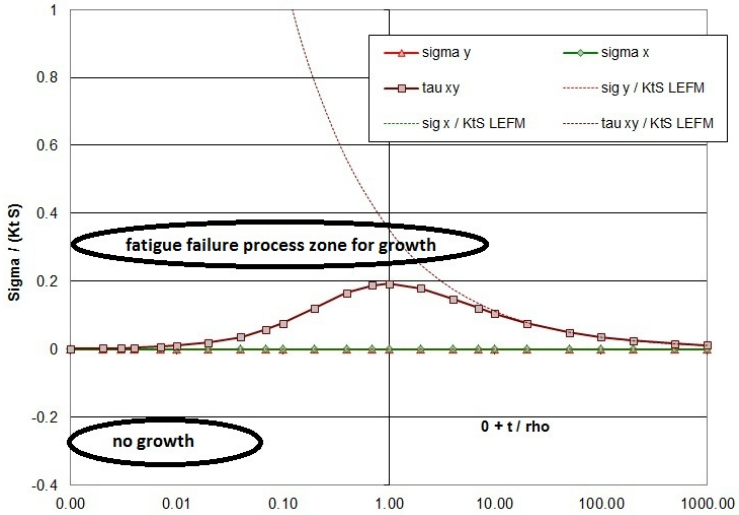

Figure 8: Mode II stresses ahead of the crack tip in pure shear, showing a small fatigue failure process zone that is too small for propagation, and a large fatigue failure process zone that permits growth. Here Λ = -1, α = 45^O, ϕ = 0^O, **D** = 10 mm, **b** = 0.001 mm, and **rho** = 10^{-7} mm.

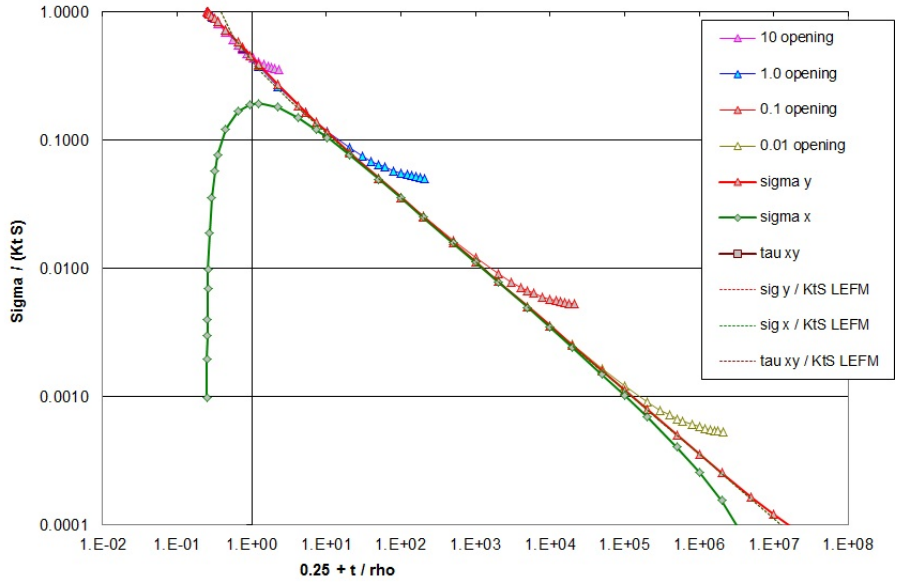

Figure 9: Mode I stresses ahead of the crack tip, for different radii of curvature. Here $\Lambda = 0$, $\alpha = 90^{O}$, $\phi = 0^{O}$, **D** = 10 mm, **b** = 0.001 mm, **rho** = 10^{-7} mm, for **sigma y, sigma x,** and **tau xy**. Results for **sigma y** only are shown for **b** = 10, 1.0, 0.1 and 0.01 mm. Note all fracture mechanics results lie on a straight line of slope -0.5. The stress **tau xy** is of course zero, from symmetry.

So for successful shear mode crack growth, one should control the sharpness of the crack tip to ensure the fatigue failure process zone is sufficiently large to generate a satisfactory stress intensity. Secondly, a mechanism to reduce friction between sliding crack faces is essential, as discussed in the Introduction.
Finally real cracks are rarely mathematically flat, and roughness induced closure is frequently sufficient to prevent sliding deformation at the crack tip. Some of the complications of rough and three-dimensional fracture surfaces are reviewed by Miller et al. [7].

REFERENCES

[1] A. Otsuka, H. Sugawara, M. Shomura, In: 4th International Conference on Biaxial/Multiaxial Fatigue, edited by A. Pineau, G. Cailletaud and T. C. Lindley, Soc. Francaise Metall. Mater., Paris, (1994) 545.
[2] S.L. Wong, P.E. Bold, M.W. Brown, R.J. Allen, Fatigue Fract. Engng. Mater. Struct., 12 (2000) 667.
[3] M.W. Brown, K.J. Miller, U.S. Fernando, J.R. Yates, D.K. Suker, In: Multiaxial Fatigue and Design, edited by A. Pineau, G. Cailletaud and T. C. Lindley, Mechanical Engineering Publications, ESIS Publication No. 21 (1996) 317.
[4] C.E. Inglis, Trans. Inst. Naval Architects, 55 (1913) 219.
[5] G.N. Savin, Stress Concentration Around Holes, Pergamon Press (1961).
[6] S.T. Xiao, M.W. Brown, K.J. Miller, Fatigue Fract. Engng. Mater. Struct., 8 (1985) 349.
[7] KJ. Miller, M.W. Brown, J.R. Yates, In: Mixed-Mode Crack Behaviour, ASTM STP 1359, edited by K.J. Miller and D.L. McDowell, American Society for Testing and Materials, (1999) 229.